Available online at www.sciencedirect.com
ScienceDirect
Journal of Computational Physics 218 (2006) 451–459
JOURNAL OF COMPUTATIONAL PHYSICS
www.elsevier.com/locate/jcp

Short note

A note on the conservative schemes for the Euler equations

Huazhong Tang [a,*], Tiegang Liu [b]

[a] LMAM, School of Mathematical Sciences, Peking University, Beijing 100871, PR China
[b] Institute of High Performance Computing, #01-01 The Capricorn, Singapore Science Park II, Singapore 117528, Singapore

Received 6 February 2006; received in revised form 21 March 2006; accepted 31 March 2006
Available online 24 May 2006

Abstract

This note gives a numerical investigation for the popular high resolution conservative schemes when applied to inviscid, compressible, perfect gas flows with an initial high density ratio as well as a high pressure ratio. The results show that they work very inefficiently and may give inaccurate numerical results even over a very fine mesh when applied to such a problem. Numerical tests show that increasing the order of accuracy of the numerical schemes does not help much in improving the numerical results. How to cure this difficulty is still open.

Keywords: High resolution schemes; Godunov scheme; The Euler equations; Rarefaction wave; Shock wave

1. Introduction

The popular high resolution conservative schemes such as the total variation diminishing (TVD) schemes, the essentially non-oscillatory (ENO) schemes or the weighted essentially non-oscillatory (WENO) schemes can usually achieve higher-order accuracy with sharp and essentially non-oscillatory shock transition. These schemes have generally been shown their robustness and worked very successfully in solving hyperbolic conservation laws for single phase compressible gas flows. However, when these schemes are applied to Riemann problems with initial large density and pressure ratios, it is found that they may fail to provide accurate numerical results, especially the position of the shock front, even over a very fine mesh. Such high density and pressure ratio problems are usually encountered in strong explosions and nuclear fusions. We have tested various high resolution schemes such as Godunv scheme [1], Roe scheme [6] with a piecewise linear reconstruction, the HLL (Harten, Lax, and van Leer) approximate Riemann solver [8] with a piecewise linear reconstruction, WENO scheme [4], gas-kinetic scheme [11], the modified ghost fluid method (MGFM) [2], and the Runge–Kutta discontinuous Galerkin (RKDG) method [3,10] as well as the space-time conservative method [5], etc. All these schemes have similar defects when applied to such a problem.

* Corresponding author. Tel.: +86 10 62757018; fax: +86 10 62751801.
E-mail addresses: hztang@math.pku.edu.cn (H. Tang), liutg@ihpc.a-star.edu.sg (T. Liu).

0021-9991/$ - see front matter
doi:10.1016/j.jcp.2006.03.035

2. Numerical experiments

Consider one-dimensional Euler equations

$$\frac{\partial U}{\partial t}+\frac{\partial F}{\partial x}=0, \tag{1}$$

where the conservative variables U and the flux $F(U)$ is defined by

$$U=[\rho,\rho u,E]^{\mathrm{T}},\quad F=[\rho u,\rho u^2+p,u(E+p)]^{\mathrm{T}}.$$

Here, u is the flow velocity, ρ is the flow density and p is the flow pressure; the flow total energy E is given as $E=\rho e+\frac{1}{2}\rho u^2$, where e denotes the internal energy per unit mass. We will limit our attention to the ideal gas only, which is constituted with the perfect gas law given as $p=(\gamma-1)\rho e$. Here, γ is the ratio of the specific heats and taken as a constant with a value of 1.4 in the present computations.

Example 2.1. The first example to be considered is a Riemann problem of (1) subject to the following initial data

$$(\rho,u,p)=\begin{cases}(1000,\ 0,\ 1000) & \text{if } 0\leqslant x<0.3,\\ (1,\ 0,\ 1) & \text{if } 0.3<x\leqslant 1.\end{cases} \tag{2}$$

This is a problem with high density and high pressure ratios given initially. As a result, there is a very strong rarefaction wave generated in the high pressure region once the diaphragm is removed. Figs. 1 and 2 show the densities and velocities at $t=0.15$ computed by using the first-order accurate Godunov scheme [1] and KFVS (kinetic flux-vector splitting) scheme [11] with CFL number of 0.32, and 100 and 2500 uniform cells, respectively. The exact solution is also shown for comparison and indicated with solid lines. The sonic point glitch [7] may be observed in the Godunov solutions; the discontinuities are not well-resolved. Fig. 3 gives the comparison between the exact and computed velocities at $t=0.15$ by the high-resolution MUSCL (Monotone Upstream Schemes for Conservation Laws) type LLF (local Lax-Friedriches) scheme with the third-order TVD Runge–Kutta time discretization over 500, 5000, 10,000, 14,000 mesh cells, respectively. We see that the intermediate state of the velocity is incorrect when grid resolution is low, e.g. with 500 cells. The close-up of the velocities given in Fig. 4 tells us further that the location of the computed shock front is still not in accordance with the exact one, even though a very fine mesh has been used.

We also checked the performances of other high-resolution conservative schemes for the above problem, which are a second-order accurate MUSCL type Roe scheme, a second-order accurate BGK scheme [11], and a fifth-order accurate WENO scheme [4]. Figs. 5–7 show the close-up of the respective velocities calculated in

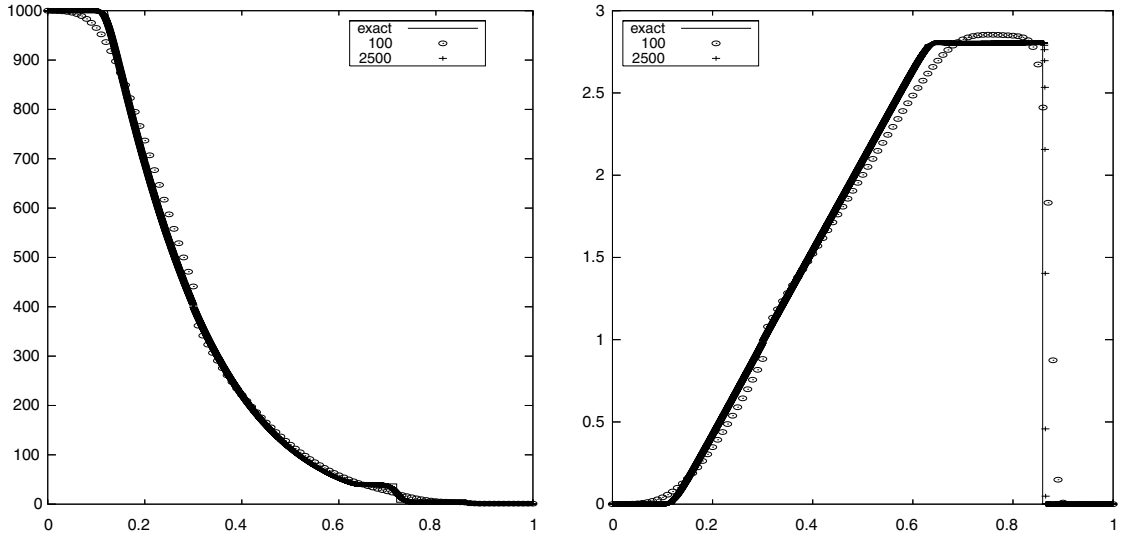

Fig. 1. Example 2.1: The results via the first-order Godunov method with CFL = 0.32. Left: the density; right: the velocity.

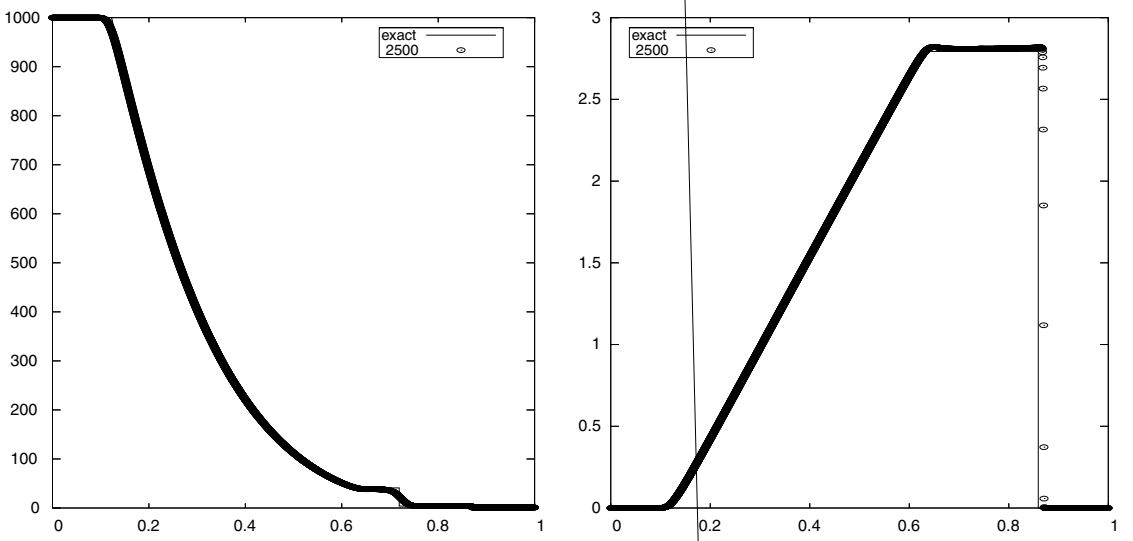

Fig. 2. Example 2.1: The results via the first-order KFVS method with CFL = 0.32. Left: the density; right: the velocity.

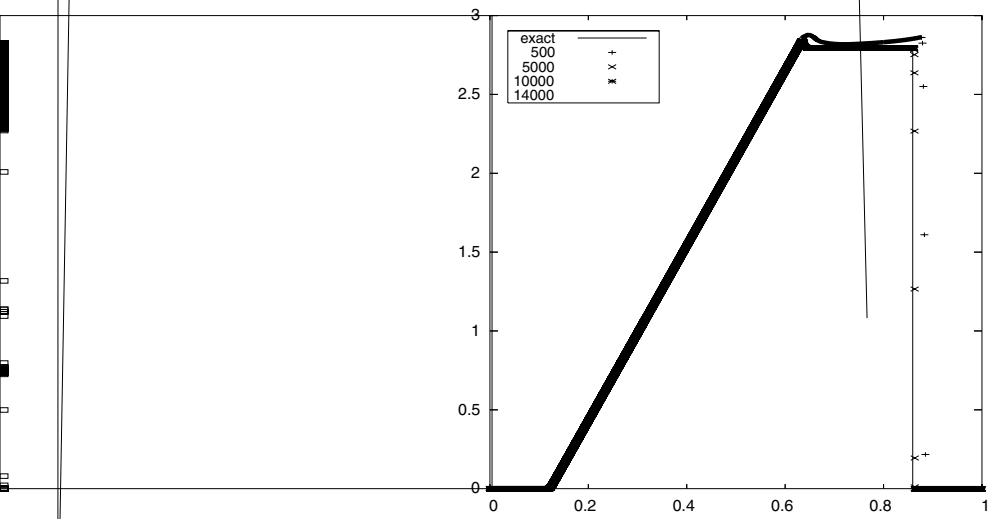

Fig. 3. Example 2.1: The velocity obtained by the MUSCL-LLF method with the minmod limiter and a third-order RK time discretization with CFL = 0.8.

the vicinity of the shock wave. We observe that the computed shock position is still inaccurate even though we have use a higher-order accurate scheme as well as a very fine mesh. This shows that increasing the order of accuracy of the scheme does not contribute much to improving the numerical results. It may be noted that among the schemes investigated, the performance of the BGK scheme is much better than others probably due to its special strategy of constructing the numerical flux. The numerical smearing at the contact discontinuity may theoretically affect the accuracy of the results. To eliminate this influence, we re-computed the problem using the MGFM-based MUSCL-HLL algorithm [2] with the exact solution to define the ghost fluid status and pressure and velocity continuity imposed at the interface [9]. Fig. 8 shows the close-up of velocities obtained by the MGFM algorithm in the vicinity of the shock front over 500, 1000 and 5000 mesh cells. The results show that the performance of the MGFM algorithm is similar to the high resolution conservative schemes. We have also investigated the behavior of the traditional Lagrange method applied to this problem. Fig. 9 shows the close-up of the velocities obtained by the Lagrange method with the Neumann–Richtmyer

artificial viscosity, and 500, 2000, 5000, and 20,000 cells used, respectively. The same phenomenon is observed too; when the number of the grid points is very large, the numerical shocks are found to lag behind the exact one. The results of both the MGFM and Lagrange method strongly imply that the mentioned defect does not attribute much to the numerical smearing at the contact discontinuity. Even for the popular DG method, similar defect is observed as shown in Fig. 10, which is obtained using the 3rd TVD Runge–Kutta DG method with the third-order spatial accuracy, where the CFL number is taken to be 0.18 and the TVB limiter is used.

Example 2.2.

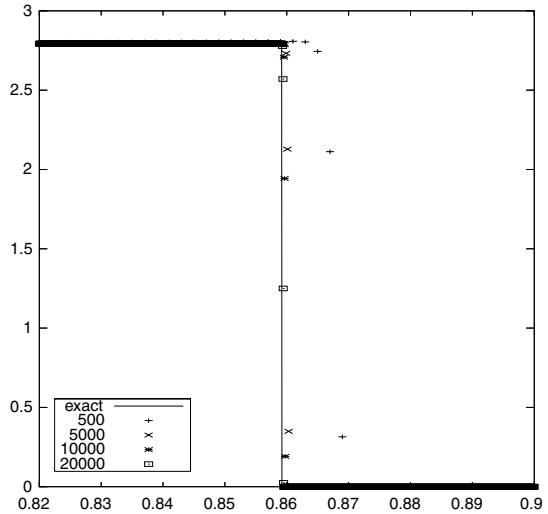

Fig. 6. Example 2.1: Close-up of the velocities calculated by the BGK method with the van Leer limiter with CFL = 0.9, and 500, 5000, 10,000, 20,000 cells, respectively.

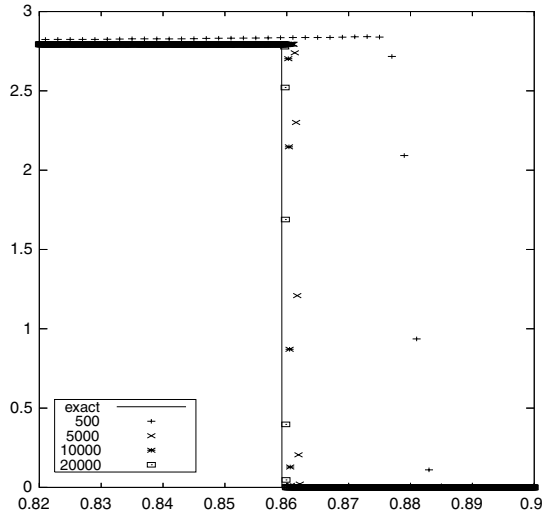

Fig. 7. Example 2.1: Close-up of the velocities calculated by the fifth-order WENO method with CFL = 0.9, and 500, 5000, 10,000, 20,000 cells, respectively.

Fig. 11 gives the comparison between the exact and computed velocities at $t = 0.12$ by using the fifth-order accurate WENO scheme with 2000, 20,000, and 200,000 cells, respectively. It is observed that the discrepancy of the shock location between the computed and exact solution becomes even large. Such a phenomenon also occurs to other high resolution schemes as well as the MGFM and RKDG methods. In all, with the further increase of density and pressure ratios, the efficiency and accuracy of the above mentioned schemes become even worse.

Example 2.3. The final example is also a shock tube problem subject to the initial data as

$$(\rho, u, p) = \begin{cases} (445,\ 0,\ 1000) & \text{if } 0 \leqslant x < 0.6, \\ (500,\ 0,\ 1) & \text{if } 0.6 < x \leqslant 1. \end{cases} \tag{4}$$

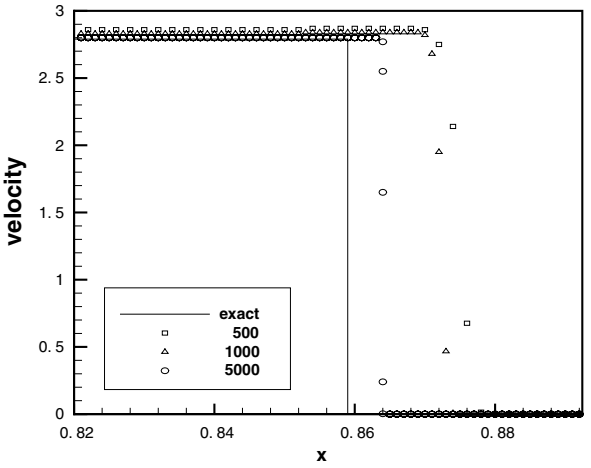

Fig. 8. Example 2.1: Close-up of the velocities calculated by the MGFM method with CFL = 0.9, and 500, 1000 and 5000 cells, respectively.

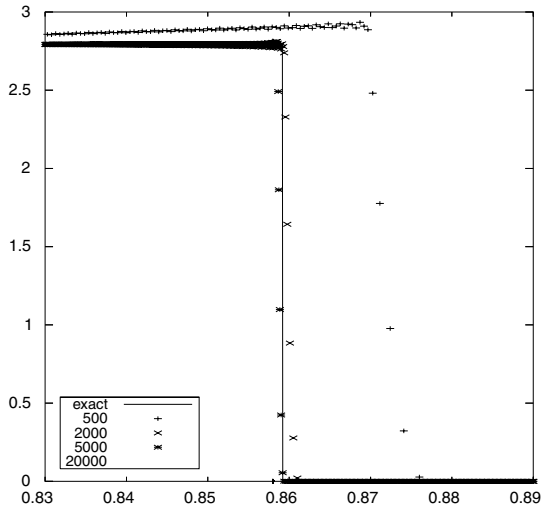

Fig. 9. Example 2.1: Close-up of the velocities calculated by the Lagrange method with the Neumann–Richtmyer artificial viscosity with CFL = 0.45, and 500, 2000, 5000, and 20,000 cells, respectively.

This problem is also considered as high pressure problem, but the density ratio is low and the shock wave is relatively much stronger. The computed and exact solutions at $t = 0.3$ are given in Fig. 12. The computed solution is obtained using the BGK scheme with 500 cells and the CFL number of 0.9. We see that the captured shock wave is correct. In fact, we have found that the inefficient performance of the high resolution schemes occurs only to those shock tube problems with a relative very strong rarefaction wave.

3. Discussion and conclusions

We have found that the popular high resolution conservative schemes worked very inefficiently for those shock tube problems with initial high pressure and high density ratios. We found that increasing scheme accuracy did not improve the results much and the numerical smearing at the contact discontinuity did not attribute much to this defect. To further understand the underlying reasons of causing this defect, we computed Example 2.1 again via using the exact solution as the initial conditions. Fig. 13 presents the close-up of

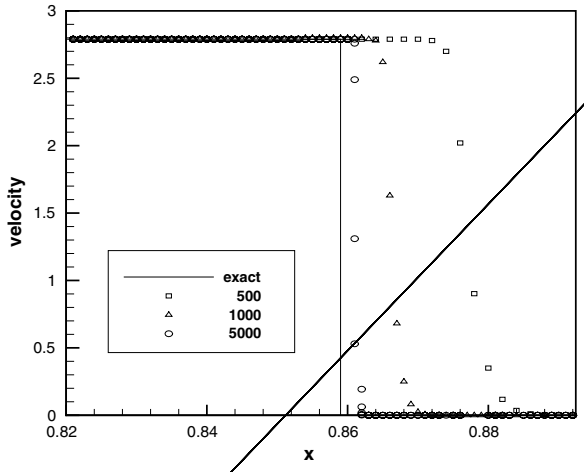

Fig. 10. Example 2.1: Close-up of the velocities calculated by the third-order RKDG method with CFL = 0.18 and 500, 1000, 5000 cells, respectively.

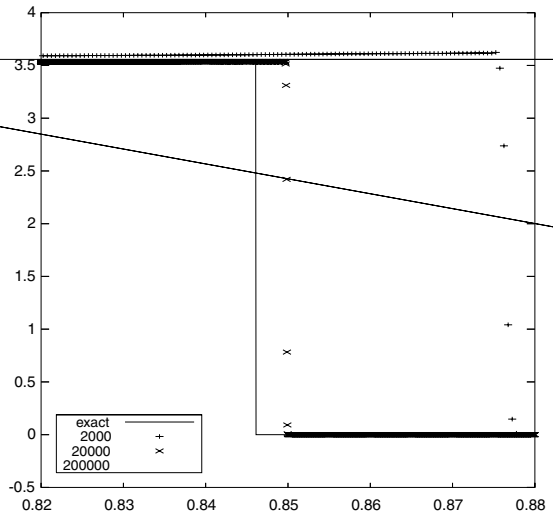

calculated velocities via using the exact solution of $U(x,t_0) = U^R(x,t_0)$ as the initial conditions at $t_0 = 0.001, 0.005, 0.006, 0.007, 0.01$, respectively. Here, $U^R(x,t_0)$ denotes the exact solution of Example 2.1 at $t = t_0$. The numerical solutions are calculated using the fifth-order accurate WENO method with CFL = 0.9 and 800 cells used. From Fig. 13, one can easily observe that the computed shock location is not correct if t_0 is taken to be 0.001, while other numerical results are correct if t_0 is taken beyond 0.001. If we project the exact solution at $t = t_0$ to the mesh used, we found that the rarefaction fan and the shock front can be resolved with 800 cells only after $t_0 > 0.001$. In fact, we have found that no matter how fine the mesh is, there is always a critical t_{cr}, which is closely related to the mesh size, such that the high resolution schemes are unable to provide the correct shock location if the exact solution of $t_0 < t_{cr}$ is used as the initial conditions. That is to say, if the given t_0 is taken to be less than t_{cr}, it is found that the rarefaction fan and the shock wave cannot be resolved by the mesh used. Thus, we can conclude that the found defect is due to the inability of the high resolution schemes to provide an earlier accurate decomposition of the initial discontinuities (singularities) if there is a very strong rarefaction wave. However, we are unable to affirm if this defect

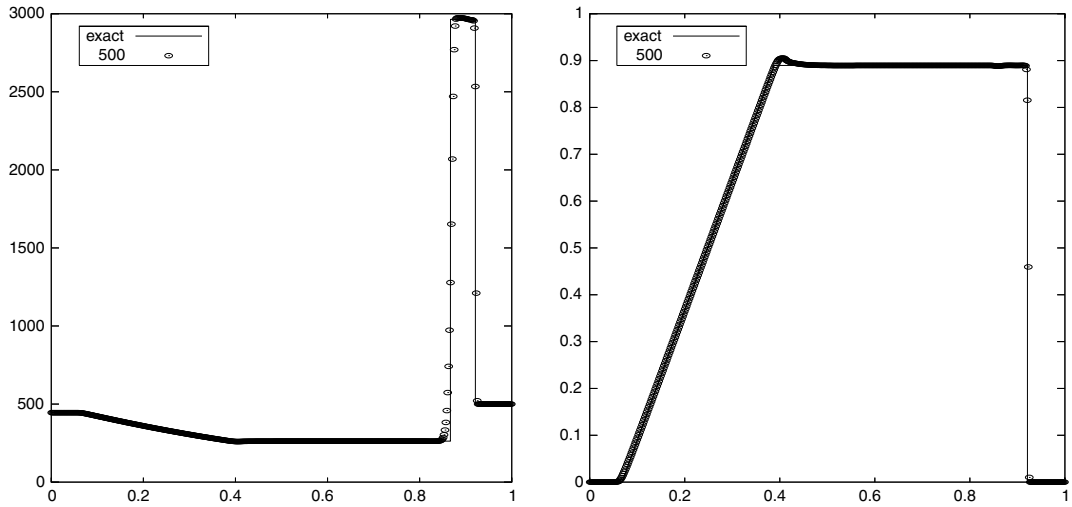

Fig. 12. Example 2.3: The results obtained by the second-order BGK method with CFL = 0.9 and 500 cells. Left: the density; right: the velocity.

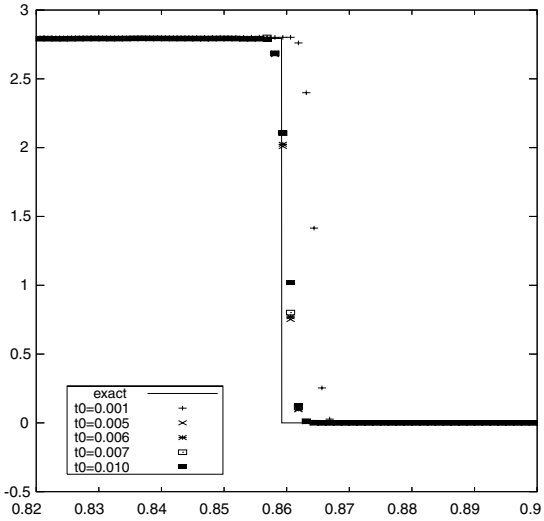

Fig. 13. Example 2.1: Close-up of the velocities subject to the initial data $U^R(x, t_0)$ and calculated by the fifth-order WENO method with CFL = 0.9 and 800 cells at $t_0 = 0.001$, 0.005, 0.006, 0.007, and 0.010, respectively.

is caused by the inaccurate decomposition of the rarefaction wave alone or the shock wave alone or both from the computation. Even if the defect could be caused solely by the inaccurate decomposition of the rarefaction wave as suspected by one of the referees of this paper, we still do not know how this inaccurate decomposition finally affects the propagation of the shock wave, leading to the entire lower resolution of numerical results over a reasonably fine mesh and the inaccurate shock location provided. Furthermore, how to cure this defect found in this work is still open.

Acknowledgements

HZT was partially supported by the National Basic Research Program under the Grant 2005CB321703, the National Natural Science Foundation of China (Nos. 10431050, 10576001), and Laboratory of Computational Physics. L.T.G. thanks Professor Qiu Jianxian providing the 1D DG codes and Professor Shen Zhijun

for the useful discussion. The authors also thank the reviewers' valuable suggestions during the revision of the paper.

References

[1] S.K. Godunov, A finite difference method for the computation of discontinuous solutions of the equations of fluid dynamics, Mat. Sb. 47 (1959) 271–306.
[2] T.G. Liu, B.C. Khoo, K.S. Yeo, Ghost fluid method for strong shock impacting on material interface, J. Comput. Phys. 190 (2003) 651–681.
[3] J. Qiu, C.-W. Shu, Runge–Kutta discontinuous Galerkin method using WENO limiters, SIAM J. Sci. Comput. 26 (2005) 907–929.
[4] G.S. Jiang, C.W. Shu, Efficient implementation of weighted ENO scheme, J. Comput. Phys. 126 (1996) 202–228.
[5] S. Qamar, G. Warnecke, A space-time conservative method for hyperbolic systems with stiff and non stiff source terms, Commun. Comput. Phys. 1 (2006) 451–480.
[6] P.L. Roe, Approximate Riemann solvers, parameter vectors, and difference schemes, J. Comput. Phys. 43 (1981) 357–372.
[7] H.Z. Tang, On the sonic point glitch, J. Comput. Phys. 202 (2005) 507–532.
[8] E.F. Toro, Riemann Solvers and Numerical Methods for Fluid Dynamics, A Practical Introduction, Springer, Berlin, 1999.
[9] C.W. Wang, T.G. Liu, B.C. Khoo, A real-ghost fluid method for the simulation of multi-medium compressible flow, SIAM Sci. Comput. 28 (2006) 278–302.
[10] Y.L. Xing, C.W. Shu, A new approach of high order well-balanced finite volume WENO schemes and discontinuous Galerkin methods for a class of hyperbolic systems with Source Terms, Commun. Comput. Phys. 1 (2006) 100–134.
[11] K. Xu, Gas-Kinetic Schemes for Unsteady Compressible Flow Simulations, VKI Fluid Dynamics Lecture Series, 1998-03, 1998.